



Известия Саратовского университета. Новая серия. Серия: Математика. Механика. Информатика. 2026. Т. 26, вып. 1. С. 81–90

*Izvestiya of Saratov University. Mathematics. Mechanics. Informatics*, 2026, vol. 26, iss. 1, pp. 81–90  
<https://mmi.sgu.ru>

DOI: <https://doi.org/10.18500/1816-9791-2026-26-1-81-90>

EDN: <https://elibrary.ru/ONOUJV>

Article

## Characterization of properties for modern dental materials and bordering tissues. Part 2. Microgeometrical properties

E. V. Sadyrin<sup>✉</sup>, A. L. Nikolaev, I. Yu. Zabayaka, S. S. Volkov

Don State Technical University, 1 Gagarin Sq., Rostov-on-Don 344003, Russia

**Evgeniy V. Sadyrin**, [esadyrin@donstu.ru](mailto:esadyrin@donstu.ru), <https://orcid.org/0009-0000-2227-1299>, SPIN: 7472-7963, AuthorID: 770513

**Andrey L. Nikolaev**, [andreynicolaev@eurosites.ru](mailto:andreynicolaev@eurosites.ru), <https://orcid.org/0000-0003-3491-4575>, SPIN: 8183-3370, AuthorID: 968623

**Igor Yu. Zabayaka**, [zabayakaigor@gmail.com](mailto:zabayakaigor@gmail.com), <https://orcid.org/0000-0001-6759-549X>, SPIN: 8599-3508, AuthorID: 922738

**Sergei S. Volkov**, [fenix\\_rsu@mail.ru](mailto:fenix_rsu@mail.ru), <https://orcid.org/0000-0001-7252-4522>, SPIN: 6349-1960, AuthorID: 740654

**Abstract.** Today, dental materials face a number of requirements related to the need to withstand to withstand high masticatory loads, while forming, while forming a strong interface with the surrounding biological tissues. The study of the microgeometrical properties of modern materials used to treat caries allows us to draw a conclusion about their efficacy in imitating the tooth tissues and and forming an interface devoid of various microdefects. In the present work, for this purpose, an *ex vivo* study of the surfaces of composite and glass ionomer cement filling sections, as well as enamel after polymer infiltration and tissues in their vicinity, was carried out using atomic force and scanning electron microscopy. The obtained roughness parameter values for areas after dental treatment were compared with those of sound tissues; one-way analysis of variance was used to assess statistically significant differences between the mean values of the studied characteristics. The results of the measurements allow us to conclude that the polymer infiltration into the tooth tissue was successful, and in the case of clinical need for filling, the composite material is preferable to glass ionomer cement.

**Keywords:** enamel, dentine, composite material, glass ionomer cement, polymer infiltrant, atomic force microscopy, microstructure, roughness

**Acknowledgements:** This work was supported by the Russian Science Foundation (project No. 25-29-00829, <https://rscf.ru/en/project/25-29-00829/>). The authors thank S. Yu. Maksyukov for assistance in performing *ex vivo* sealing of the samples. Atomic force and scanning electron microscopy were carried out using the equipment of the Resource Center for Collective Use of the Scientific and Educational Center for Functional Gradient Materials of Don State Technical University (RCCP DSTU).

**For citation:** Sadyrin E. V., Nikolaev A. L., Zabayaka I. Yu., Volkov S. S. Characterization of properties for modern dental materials and bordering tissues. Part 2. Microgeometrical properties. *Izvestiya of Saratov University. Mathematics. Mechanics. Informatics*, 2026, vol. 26, iss. 1, pp. 81–90. DOI: <https://doi.org/10.18500/1816-9791-2026-26-1-81-90>, EDN: ONOUJV

This is an open access article distributed under the terms of Creative Commons Attribution 4.0 International License (CC-BY 4.0)



Научная статья  
УДК 531.7

## Характеризация свойств современных стоматологических материалов и тканей в их окрестности.

### Часть 2. Микрогеометрические свойства

Е. В. Садырин<sup>✉</sup>, А. Л. Николаев, И. Ю. Забияка, С. С. Волков

Донской государственный технический университет, Россия, 344003, г. Ростов-на-Дону, пл. Гагарина, д. 1

**Садырин Евгений Валерьевич**, кандидат физико-математических наук, старший научный сотрудник лаборатории механики биосовместимых материалов, доцент кафедры «Теоретическая и прикладная механика», esadyrin@donstu.ru, <https://orcid.org/0009-0000-2227-1299>, SPIN: 7472-7963, AuthorID: 770513

**Николаев Андрей Леонидович**, заведующий лабораторией механики биосовместимых материалов, andreynicolaev@eurosites.ru, <https://orcid.org/0000-0003-3491-4575>, SPIN: 8183-3370, AuthorID: 968623

**Забияка Игорь Юрьевич**, младший научный сотрудник лаборатории электронной и оптической микроскопии, zabiyaikaigor@gmail.com, <https://orcid.org/0000-0001-6759-549X>, SPIN: 8599-3508, AuthorID: 922738

**Волков Сергей Сергеевич**, ведущий научный сотрудник лаборатории функционально-градиентных и композиционных материалов, fenix\_rsu@mail.ru, <https://orcid.org/0000-0001-7252-4522>, SPIN: 6349-1960, AuthorID: 740654

**Аннотация.** На сегодняшний день к стоматологическим материалам выдвигается ряд требований, связанных с необходимостью выдерживать высокую нагрузку при пережевывании пищи, при этом формируя прочную границу раздела с окружающей биологической тканью. Исследование микрогеометрических свойств современных материалов, используемых для лечения кариеса, позволяет сделать вывод о том, насколько они способны эффективно имитировать ткань зуба и формировать интерфейс, лишённый разного рода микродефектов. В настоящей работе для данной цели проведено *ex vivo* исследование поверхностей шлифов пломб из композитного материала и стеклоиномерного цемента, а также эмали после полимерной инфильтрации и тканей в их окрестности с использованием атомно-силовой и сканирующей электронной микроскопии. Полученные значения параметров шероховатости для областей после стоматологического вмешательства сравнивались со значениями для здоровых тканей, для оценки статистически значимых различий между средними значениями изучаемых характеристик использовался однофакторный дисперсионный анализ. Результаты измерений позволили сделать вывод об успешности проникновения полимерного инфильтранта в ткани зуба, при этом в случае клинической необходимости пломбирования композитный материал оказался предпочтительнее, чем стеклоиномерный цемент.

**Ключевые слова:** эмаль, дентин, композитный материал, стеклоиномерный цемент, полимерный инфильтрант, атомно-силовая микроскопия, микроструктура, шероховатость

**Благодарности:** Исследование выполнено при поддержке Российского научного фонда (проект № 25-29-00829, <https://rscf.ru/project/25-29-00829/>). Авторы благодарят С. Ю. Максуюкова за помощь в проведении *ex vivo* установки пломб на образцах. Атомно-силовая и сканирующая электронная микроскопия выполнены на оборудовании Ресурсного центра коллективного пользования НОЦ «Материалы» Донского государственного технического университета (РЦКП ДГТУ).

**Для цитирования:** Sadyrin E. V., Nikolaev A. L., Zabiyaika I. Yu., Volkov S. S. Characterization of properties for modern dental materials and bordering tissues. Part 2. Microgeometrical properties [Садырин Е. В., Николаев А. Л., Забияка И. Ю., Волков С. С. Характеризация свойств современных стоматологических материалов и тканей в их окрестности. Часть 2. Микрогеометрические свойства] // Известия Саратовского университета. Новая серия. Серия: Математика. Механика. Информатика. 2026. Т. 26, вып. 1. С. 81–90. DOI: <https://doi.org/10.18500/1816-9791-2026-26-1-81-90>, EDN: ONOUJY

Статья опубликована на условиях лицензии Creative Commons Attribution 4.0 International (CC-BY 4.0)

*Continuation.* See the beginning: *Izvestiya of Saratov University. Mathematics. Mechanics. Informatics*, 2025, vol. 25, iss. 4, pp. 555–565. DOI: <https://doi.org/10.18500/1816-9791-2025-25-4-555-565>, EDN: SRTEFP



## Introduction

The total annual national expenditure on outpatient dental care (public and private) in Russia is estimated at 892 million US dollars (as of 2019, according to [1]). The most common disease of the oral cavity is caries, the mechanisms of which are associated with the progressive loss of the mineral component of hard tissues under the influence of acidogenic bacteria in the dental biofilm. This is expressed in a decrease in mineral density, mechanical properties, and other alterations [2]. Teeth are usually in a dynamic equilibrium of alternating demineralization and remineralization, where the former is a partial dissolution of hydroxyapatite crystallites in the presence of acid, and the latter is a reprecipitation and crystallization of minerals in the tissues [3, 4]. Caries occurs in the case of prolonged demineralization, while its early manifestations (white spot stage, WSP), as a rule, occur without the formation of significant enamel defects.

Long-term demineralization of dental tissues is reflected in changes in their microstructure and microgeometrical parameters. A number of researchers [5] used optical coherence tomography to describe changes in the microstructure of biological dental tissues affected by WSLs for early diagnosis of the patient. Kiesow et al. [6] visualized changes in the microstructure and chemical composition of human enamel during treatment and remineralization of artificially created carious lesions. Besnard et al. [7] performed nano/macro-histological characterization of the hierarchical structure of human carious enamel using various techniques, including light microscopy, scanning electron microscopy (SEM), focused ion beam, and X-ray tomography. In [8], the structure and mechanical properties of pathologically altered enamel and dentine were studied using both optical microscopy and nanoindentation, and in [9], a correlation was studied between the mechanical properties and mineral density of dentine damaged by caries at the stage of brown spot lesion. Zuluaga – Morales et al. [10] assessed the effect of the *pH* cycling procedure on the mineral composition and microstructure of dentine using SEM and backscattering spectroscopy. Atomic force microscopy (AFM) is a common tool for assessing microgeometrical parameters and local microstructural features of areas susceptible to caries [11].

AFM and SEM techniques allow for the qualitative and quantitative characterization of microgeometrical parameters not only of pathologically altered tissues but also of biocompatible materials that are intended to replace or modify these tissues. Kakaboura et al. [12] conducted an *in vitro* study aimed at comparing different methods for measuring surface roughness and topography in several types of dental composite materials. Guler and Unal [13] evaluated the surface roughness parameters and color changes of five dental restorative materials after aging in liquids at different *pH* values. In [14], the morphological and structural changes in enamel after processing with an Er:YAG laser using AFM, SEM, and energy-dispersive X-ray spectroscopy were evaluated.

In the present work, an *ex vivo* study of the microgeometrical properties of composite and GIC fillings, the enamel surrounding these fillings, the dentine in their vicinity (i.e., located as close as possible to the dentine-enamel junction close to the filling, DEJ), and sound dentine and enamel on the opposite side of the tooth was performed using AFM. A similar scheme was used to study the mechanical and microgeometrical properties of enamel modified with an infiltrant and the dentine in its vicinity, as well as sound tissues. This approach ensured not only a quantitative assessment of the values of microgeometrical characteristics in areas that are key for a dental clinician, but also a visual comparison of the results of dental intervention. For a more detailed interpretation of the obtained experimental data, SEM images of the areas of interest were obtained.

## 1. Materials and methods

The study included four human molars extracted for orthodontic reasons in the Dental Department of the Rostov State Medical University Clinic, Rostov-on-Don, Russia. The local independent ethics committee of the university approved the study protocol (extract 14/21 dated September 23, 2021), and the patients provided informed consent. The dental materials



used in the samples included Vitremer glass ionomer cement (GIC) (3M ESPE, St. Paul, USA), Estelite Flow Quick composite (Tokuyama Dental, Tokyo, Japan), and Icon infiltrant (DMG Chemisch-Pharmazeutische, Berlin, Germany). To form thin sections of the surface of the samples containing the areas under study, their sample preparation was performed in longitudinal section using an Isomet 4000 precision saw (Buehler, Lake Bluff, USA), then grinding (with SiC-based sandpaper of P800, P1200, P2000, P2500 grain size) and polishing the surface (diamond particles with a diameter of 6 and 1  $\mu\text{m}$ , final polishing was performed using a sol-gel suspension containing aluminum oxide particles with a diameter of 0.05  $\mu\text{m}$ ) on a glass substrate.

The study of the microgeometrical characteristics of the sample surface was carried out on an AFM Nanoeducator (NT-MDT, Zelenograd, Russia) equipped with a tungsten probe. Scanning was performed in a semi-contact mode at a speed of 10.05  $\mu\text{m/s}$  at a resolution of 256 x 256 pixels. The probe was positioned using an optical USB microscope installed above the force interaction sensor of the device. Gwyddion software (Czech Metrology Institute, Brno, Czech Republic) was used for image processing. The microgeometrical characteristics (average surface roughness  $R_a$  and average maximum profile height  $R_z$ ) were measured in three directions: horizontal, vertical, and diagonal ones. Five profiles were constructed for each of these directions, and each profile was considered as an average of 10 adjacent profiles. Thus, the average value of 150 profiles with a standard deviation was then obtained. The maximum roughness height  $R_t$  was measured for the entire image.

Visualization of the filling surfaces and the interfaces between the filling and the surrounding enamel was performed using a Crossbeam 340 SEM (Carl Zeiss Microcracy GmbH, Oberkochen, Germany). Before the examination, the tooth samples were successively kept in baths with acetone solutions (pure for analysis) of 25, 50 and 70% (by volume) for 5 min each, then 80, 90, 95 and 100% (by volume) for 15 min each and, finally, were successively immersed twice in 100% (by volume) acetone for 30 min, and finally in 100% (by volume) acetone for 48 hours at 4 °C. The samples were then kept in a vacuum chamber for 1 hour at a pressure of  $6 \times 10^{-2}$  mbar, then 1 hour at a pressure of  $5 \times 10^{-2}$  mbar, then 24 hours at a pressure of  $2 \times 10^{-2}$  mbar until the pressure reached  $6 \times 10^{-1}$  mbar. SEM studies were performed using an Everhart–Thornley secondary electron detector with an accelerating voltage of 1 kV. The aperture size was 30  $\mu\text{m}$ .

The Shapiro–Wilk test was used to test whether the sets of microgeometrical characteristics were normally distributed. The test statistic ( $D$ ) provided a measure of how much the data set distribution deviated from the normal distribution. The  $p$  value quantified this probability. One-way analysis of variance (ANOVA) was used to identify statistically significant differences between the means of the two study groups of  $R_a$  (before and after dental treatment) for each sample. In particular, the null hypothesis was tested:  $H_0 : \mu_1 = \mu_2 = \dots = \mu_k$ , where  $\mu$  is the group mean, and  $k$  is the number of groups. The  $F$ -coefficient at a significance level of  $\alpha = 0.05$  was used in the calculations.

## 2. Results and discussion

Figures 1, 2 show AFM images demonstrating characteristic micro- and nanoscale structural features for each region of interest of the sample over a scanning field of  $8 \times 8 \mu\text{m}$ . The microgeometrical roughness parameters calculated from these images are given in the Table.

Figure 3 shows the surface profiles of the pores of the composite material from Fig. 1, *a* (averaging over 20 adjacent profiles) and the GIC particle (averaging over 40 adjacent profiles) from Fig. 1c, indicated by the dotted line. The roughness parameter values according to the profilograms for the pores of the composite material were 23.6, 106.8, 130.2 nm; for a typical glass particle — 103.7, 323.3, 396.0 nm for  $R_a$ ,  $R_z$ ,  $R_t$ , respectively.

To assess statistically significant differences in the results of microgeometrical measurements, two sets of  $R_a$  values were selected (sample size — 15 measurements for each): composite filling and sound enamel; GIC filling and sound enamel; infiltrated enamel and sound enamel (for two cases). In all cases, we obtained from the sample information that the test statistic  $F$  is not in



the 95% acceptance region, based on which a conclusion was made to reject the null hypothesis (at a  $p$  value  $< 0.05$ ), thus, at least two group mean values for each material were statistically significantly different from each other.

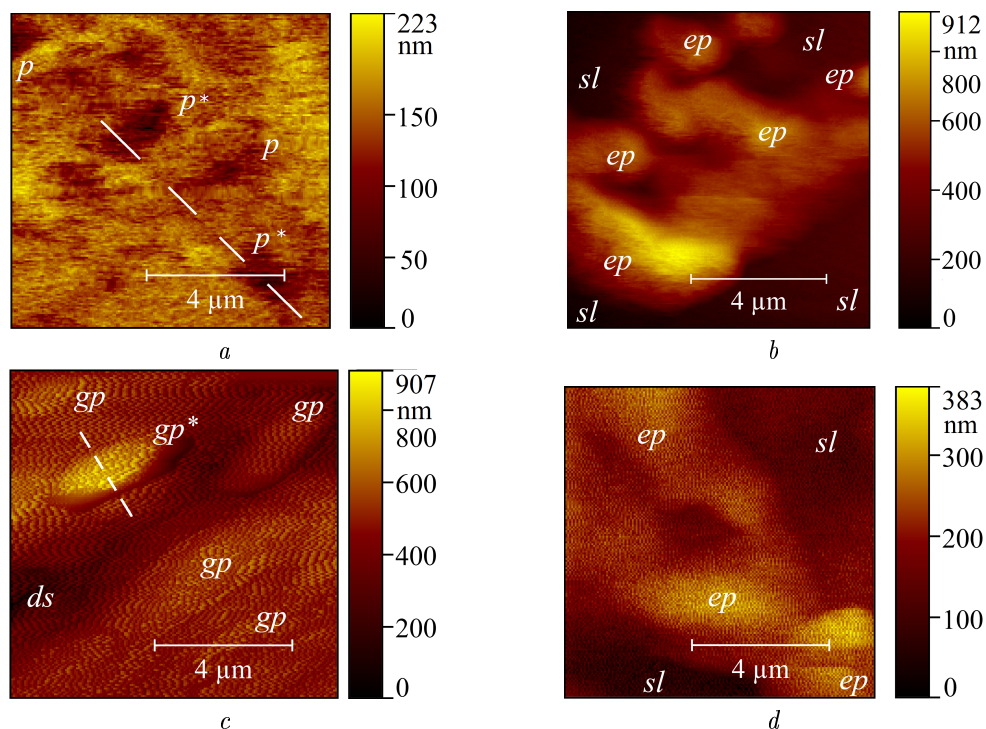


Fig. 1. Typical AFM determined topography of the surface areas: *a, b* shows composite filling and sound enamel; *c, d* shows GIC filling and sound enamel; *ep* stands for enamel prism, *p* stands for pore, *sl* stands for smear layer, *gp* stands for glass particle, *ds* stands for debonding surface; the symbol \* denotes relief elements for which separate surface profilograms were constructed (color online)

Table. Microgeometrical properties of the samples studied

Treatment type	Goup	$R_a$ , nm	$\pm$	$R_z$ , nm	$\pm$	$R_t$ , nm
Composite filling	Filling	18.0	3.2	72.1	18.1	223
	Sound enamel	92.8	33.6	345.5	117.9	912
GIC filling	Filling	68.2	24.9	242.6	90.0	907
	Sound enamel	39.5	10.4	132.4	45.2	383
Infiltrant (first case)	Infiltrated enamel	51.0	14.6	178.7	56.6	486
	Sound enamel	19.0	11.8	65.6	36.7	796
Infiltrant (second case)	Infiltrated enamel	53.2	20.4	203.3	82.5	619
	Sound enamel	31.8	7.6	109.5	26.5	355

Figures 4, *a, c* show the SEM images of the surfaces of composite and glass ionomer cement fillings, respectively, and Fig. 4, *b, d* show the interfaces of the above-mentioned fillings with the surrounding enamel.

The results of microgeometrical measurements of filling materials showed a fundamental difference in the nature of the roughness parameters in the pairs “filling—sound enamel” for the composite material and GIC. Thus, in the case of GIC, each value of the roughness parameter was higher than that recorded for the sound enamel:  $R_a$  by 72.7%,  $R_z$  by 83.2%,  $R_t$  by 2.1 times. This is explained by the presence of large ellipsoidal glass particles on the filling surface [15] (designated as *gp* in Fig. 1, *c* and Fig. 3), which alternate with delamination surfaces [16] (designated as *ds* in Fig. 1, *c*), forming a loose surface structure. The characteristic dimensions of the microscale



glass particles in the AFM image were: length  $3.23 \pm 0.85 \mu\text{m}$ , width  $1.17 \pm 0.27 \mu\text{m}$ . In the case of the composite material, on the contrary, the values of all the studied mechanical properties were lower for the filling compared to the sound enamel:  $R_a$  by 80.6%,  $R_z$  by 79.1%,  $R_t$  by 75.6%. This filling on the section showed the least developed relief among all the studied areas within the framework of this AFM study.

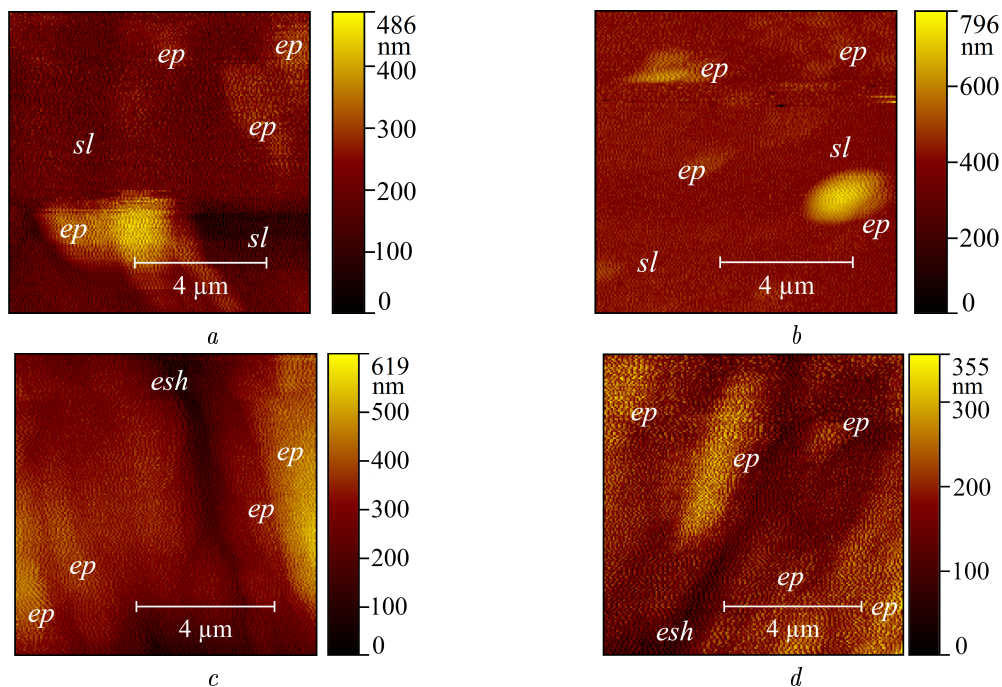


Fig. 2. Typical AFM determined topography of the surface areas: *a, b* shows infiltrated enamel (first case) — sound enamel; *c, d* shows infiltrated enamel (second case) — sound enamel; *ep* stands for enamel prism, *sl* stands for smear layer, *gp* stands for glass particle, *ds* stands for debonding surface, *esh* stands for enamel sheath (color online)

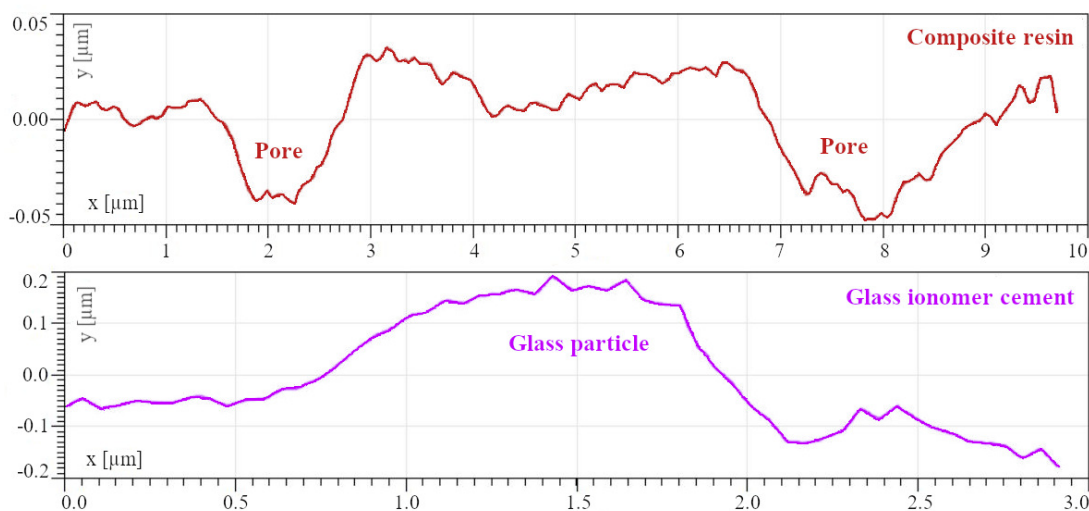


Fig. 3. Surface profiles of pores of composite material and glass particle of GIC

However, the microstructure of the composite filling has one important feature — micropores (marked as *p* in Fig. 1, *a*), typical diameters of which are  $0.86 \pm 0.25 \mu\text{m}$ . At the same time, SEM observations reveal the smallest cracks between the enamel prisms (Fig. 4, *b*), as well as in the vicinity of the GIC pores (Fig. 4, *c*). We note large-scale damage to the GIC-biological



tissue interface, clearly visible in SEM images (Fig. 4, *d*) with a width of more than  $50\ \mu\text{m}$ , presumably caused by increased stress concentration due to the excessive difference in the mechanical characteristics of the filling and the surrounding tissue (which can be further studied using the approaches [17–19]).

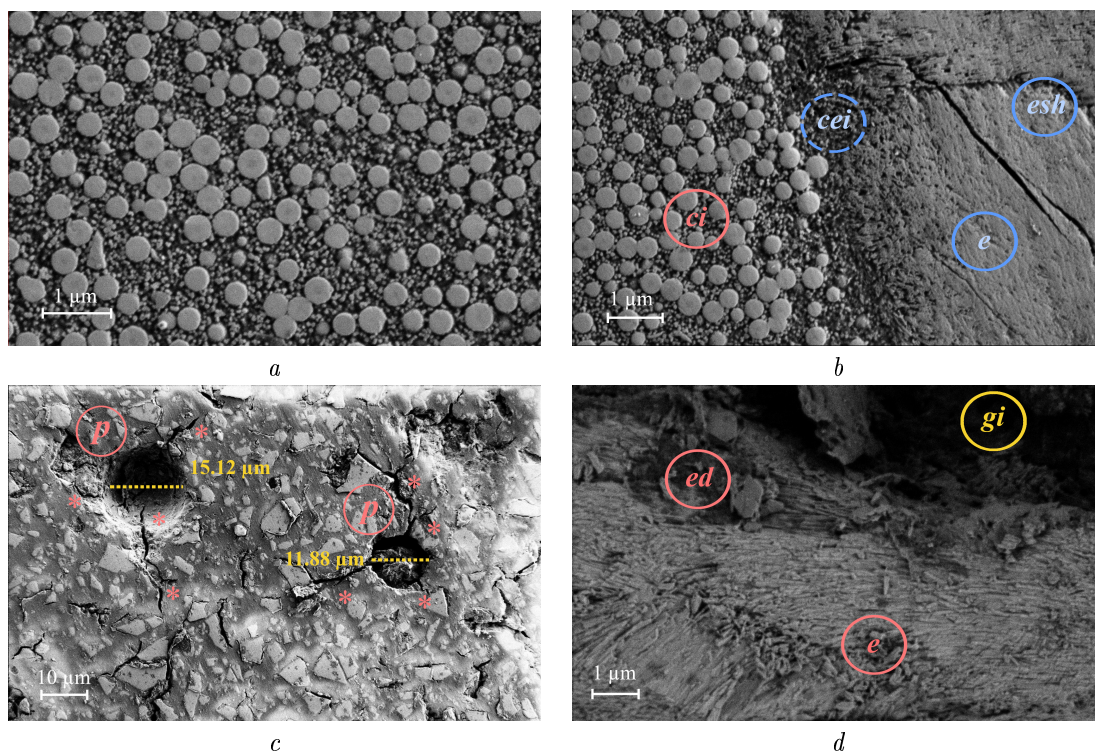


Fig. 4. Microstructure of surfaces obtained using SEM: *a* shows composite filling; *b* shows interface of the composite filling with surrounding enamel; *c* shows GIC filling; *d* shows tissue on the interface with the GIC filling; *e* stands for enamel, *ed* stands for damaged enamel, *ci* stands for inner layer of the filling, *gi* stands for interface between GIC and tissue, *cei* stands for interface between the filling and enamel, *esh* stands for enamel sheath, *p* stands for pore, symbol \* marks the cracks in the vicinity of the pores in GIC (color online)

The results of microgeometrical measurements of the infiltrant showed a generally similar picture for both samples: in both cases, an increase in the parameters  $R_a$  and  $R_z$  was recorded. For the first sample treated with the infiltrant, these roughness parameters were 2.7 times higher than in sound enamel. For the second sample, these parameters were 67.3% and 85.7% higher than in the sound enamel for  $R_a$  and  $R_z$ , respectively. Note the closeness of the absolute values of  $R_a$  and  $R_z$  for both samples after infiltration. Note also that the analysis of the parameter  $R_t$  taken over the scanning field as a whole, although providing useful information about the microrelief of the material, requires a significantly larger number of AFM images in different areas of interest to collect statistical information and form reliable conclusions about peak heights and other features of the elevated surface of the sample surface.

Changes in the microgeometrical characteristics of the samples after infiltration indicate successful penetration of the polymer infiltrant into the tissue, which is consistent with the results of Sadyrin et al. [20], while a visual similarity of the microrelief of the tissue surface before and after treatment was noted. This observation indicates that, by modifying the enamel, the infiltrant generally preserves the enamel structure relatively intact and close to natural tissue, although the mechanical properties of the tissue cannot be fully restored due to the difference in the properties of the polymer and natural hydroxyapatite.



## Conclusion

In the present work, an *ex vivo* study of the microgeometrical properties of composite and GIC fillings, as well as of infiltrated enamel and tissues in their vicinity, was performed, followed by a comparison of the results with the corresponding properties of the sound tissues. In the case of GIC, an increase in each roughness parameter value was recorded compared to the sound enamel, which is explained by the presence of large ellipsoid glass particles on the filling surface, alternating with exfoliation surfaces. In the case of the composite material, on the contrary, the values of all the studied microgeometrical properties were significantly lower for the filling compared to sound enamel, while micropores were found on its surface. The obtained experimental data allow us to conclude that in case of clinical need for filling, it is preferable to use a composite material due to a smaller number of internal structure artifacts and a smaller size of such artifacts (in addition to the proximity of the mechanical parameters of this biocompatible material to the surrounding biological tissue).

Calculations of the roughness parameters demonstrated that, although none of the materials examined restored the microgeometric characteristics to natural values, the infiltrant generally preserves the enamel microstructure. The results of the study, together with the previously made conclusions about the mineral density of enamel modified by the infiltrant [21], are encouraging in terms of the clinical use of minimally invasive dental materials; some features of the interaction of such materials and tooth tissues are still not fully understood. In particular, how does the thickness of the enamel (and proximity to the DEJ) affect the process of infiltrant penetration (e.g., which areas of the tooth are preferable for this type of treatment, and which areas should be avoided).

Despite the statistically significant difference in the mean  $R_a$  roughness values across the set of measurements in the single sample studies, in future studies, we plan to collect statistical data on the depth of infiltrate penetration into different areas of the tooth, including the DEJ, using a larger number of samples. Such further studies will provide an opportunity to develop guidelines for practicing dental clinicians on the treatment of early caries with maximum benefit for the patient, thereby expanding on existing recommendations [22–25].

## References

1. Jevdjevic M., Listl S. Economic impacts of oral diseases in 2019-data for 194 countries. *Database, Heidelberg Open Research Data* (heiDATA)[accessed 2025 May 6], 2022. DOI: <https://doi.org/10.11588/data/JGJKK0>
2. Sadyrin E., Swain M., Mitrin B., Rzhepakovsky I., Nikolaev A., Irkha V., Yogina D., Lyanguzov N., Maksyukov S., Aizikovich S. Characterization of enamel and dentine about a white spot lesion: Mechanical properties, mineral density, microstructure and molecular composition. *Nanomaterials*, 2020, vol. 10, iss. 9, art. 1889. DOI: <https://doi.org/10.3390/nano10091889>
3. Xue J., Li W., Swain M. V. *In vitro* demineralization of human enamel natural and abraded surfaces: A micromechanical and SEM investigation. *Journal of Dentistry*, 2009, vol. 37, iss. 4, pp. 264–272. DOI: <https://doi.org/10.1016/j.jdent.2008.11.020>
4. Zavgorodniy A. V., Rohanizadeh R., Swain M. V. Ultrastructure of dentine carious lesions. *Archives of Oral Biology*, 2008, vol. 53, iss. 2, pp. 124–132. DOI: <https://doi.org/10.1016/j.archoralbio.2007.08.007>
5. Shi B., Niu J., Zhou X., Dong X. Quantitative assessment methods of early enamel caries with optical coherence tomography: A review. *Applied Sciences*, 2022, vol. 12, iss. 17, art. 8780. DOI: <https://doi.org/10.3390/app12178780>
6. Kiesow A., Morawietz M., Gruner J., Gierth S., Berthold L., Schneiderman E., St John S. High-resolution characterization of enamel remineralization using time-of-flight secondary ion mass spectrometry and electron microscopy. *Caries Research*, 2024, vol. 58, iss. 4, pp. 407–420. DOI: <https://doi.org/10.1159/000535979>
7. Besnard C., Marie A., Buček P., Sasidharan S., Harper R. A., Marathe S., Wanelik K., Landini G., Shelton R. M., Korsunsky A. M. Hierarchical 2D to 3D micro/nano-histology of human dental caries



- lesions using light, X-ray and electron microscopy. *Materials & Design*, 2022, vol. 220, art. 110829. DOI: <https://doi.org/10.1016/j.matdes.2022.110829>
8. Sadyrin E. V., Yogina D. V., Vasiliev A. S., Aizikovitch S. M. Evaluation of the influence of white spot lesion on the mechanical properties of human tooth enamel and dentine. *Izvestiya of Saratov University. Mathematics. Mechanics. Informatics*, 2022, vol. 22, iss. 3, pp. 346–359 (in Russian). DOI: <https://doi.org/10.18500/1816-9791-2022-22-3-346-359>, EDN: ZTLZZQ
  9. Sadyrin E. V. Correlating the mechanical properties to the mineral density of brown spot lesion in dentine using nanoindentation and X-ray micro-tomography. In: Altenbach H., Eremeyev V. A., Galybin A., Vasiliev A. (eds.) *Advanced Materials Modelling for Mechanical, Medical and Biological Applications*. Advanced Structured Materials, vol. 155. Cham, Springer, 2022, pp. 389–398. DOI: [https://doi.org/10.1007/978-3-030-81705-3\\_21](https://doi.org/10.1007/978-3-030-81705-3_21)
  10. Zuluaga-Morales J. S., Bolaños-Carmona M. V., Cifuentes-Jiménez C. C., Álvarez-Lloret P. Chemical, microstructural and morphological characterisation of dentine caries simulation by pH-cycling. *Minerals*, 2021, vol. 12, iss. 1, art. 5. DOI: <https://doi.org/10.3390/min12010005>
  11. Coradin T., Porporatti A. L., Bosco J. Assessing *in vitro* remineralization of primary artificial caries: A systematic review of multi-techniques characterization approaches. *Dentistry Review*, 2023, vol. 3, iss. 4, art. 100073. DOI: <https://doi.org/10.1016/j.dentre.2023.100073>
  12. Kakaboura A., Fragouli M., Rahiotis C., Silikas N. Evaluation of surface characteristics of dental composites using profilometry, scanning electron, atomic force microscopy and gloss-meter. *Journal of Materials Science: Materials in Medicine*, 2007, vol. 18, iss. 1, pp. 155–163. DOI: <https://doi.org/10.1007/s10856-006-0675-8>
  13. Guler S., Unal M. The evaluation of color and surface roughness changes in resin based restorative materials with different contents after waiting in various liquids: An SEM and AFM study. *Microscopy Research and Technique*, 2018, vol. 81, iss. 12, pp. 1422–1433. DOI: <https://doi.org/10.1002/jemt.23104>
  14. Rodríguez-Vilchis L. E., Contreras-Bulnes R., Olea-Mejía O. F., Sánchez-Flores I., Centeno-Pedraza C. Morphological and structural changes on human dental enamel after Er: YAG laser irradiation: AFM, SEM, and EDS evaluation. *Photobiomodulation, Photomedicine, and Laser Surgery*, 2011, vol. 29, iss. 7, pp. 493–500. DOI: <https://doi.org/10.1089/pho.2010.2925>
  15. Xie D., Brantley W. A., Culbertson B. M., Wang G. Mechanical properties and microstructures of glass-ionomer cements. *Dental Materials*, 2000, vol. 16, iss. 2, pp. 129–138. DOI: [https://doi.org/10.1016/s0109-5641\(99\)00093-7](https://doi.org/10.1016/s0109-5641(99)00093-7)
  16. Kheur M., Kantharia N., Iakha T., Kheur S., Husain N. A. H., Özcan M. Evaluation of mechanical and adhesion properties of glass ionomer cement incorporating nano-sized hydroxyapatite particles. *Odontology*, 2020, vol. 108, iss. 1, pp. 66–73. DOI: <https://doi.org/10.1007/s10266-019-00427-5>
  17. Shahmoradi M., Wan B., Zhang Z., Swain M., Li Q. Mechanical failure of posterior teeth due to caries and occlusal wear-A modelling study. *Journal of the Mechanical Behavior of Biomedical Materials*, 2022, vol. 125, art. 104942. DOI: <https://doi.org/10.1016/j.jmbbm.2021.104942>
  18. Yilmaz E. D., Schneider G. A., Swain M. V. Influence of structural hierarchy on the fracture behaviour of tooth enamel. *Philosophical Transactions of the Royal Society A: Mathematical, Physical and Engineering Sciences*, 2015, vol. 373, iss. 2038, art. 20140130. DOI: <https://doi.org/10.1098/rsta.2014.0130>
  19. Li Y., Shao B., Liu Z. Adhesive damage of class V restorations under shrinkage stress and occlusal forces using cohesive zone modeling. *Journal of the Mechanical Behavior of Biomedical Materials*, 2025, vol. 163, art. 106880. DOI: <https://doi.org/10.1016/j.jmbbm.2024.106880>
  20. Sadyrin E. V., Yogina D. V., Swain M. V., Maksyukov S. Yu., Vasiliev A. S. Efficacy of dental materials in terms of apparent mineral density restoration: Composite resin, glass ionomer cement and infiltrant. *Composites Part C: Open Access*, 2021, vol. 6, art. 100192. DOI: <https://doi.org/10.1016/j.jcomc.2021.100192>
  21. Sadyrin E. V. Influence of a polymeric infiltrant on the density of enamel white spot lesions. *Izvestiya of Saratov University. Mathematics. Mechanics. Informatics*, 2023, vol. 23, iss. 1, pp. 83–94 (in Russian). DOI: <https://doi.org/10.18500/1816-9791-2023-23-1-83-94>, EDN: MMVQYM
  22. De Caluwé T., Vercruyse C. W. J., Fraeyman S., Verbeeck R. M. H. The influence of particle size and fluorine content of aluminosilicate glass on the glass ionomer cement properties. *Dental Materials*, 2014, vol. 30, iss. 9, pp. 1029–1038. DOI: <https://doi.org/10.1016/j.dental.2014.003>
  23. Moheet I. A., Luddin N., Ab Rahman I., Kannan T. P., Abd Ghani N. R. N., Masudi S. M.



- Modifications of glass ionomer cement powder by addition of recently fabricated nano-fillers and their effect on the properties: A review. *European Journal of Dentistry*, 2019, vol. 13, iss. 3, pp. 470–477. DOI: <https://doi.org/10.1055/s-0039-1693524>
24. Al-Halabi M., Salami A., Alnuaimi E., Kowash M., Hussein I. Assessment of paediatric dental guidelines and caries management alternatives in the post COVID-19 period. A critical review and clinical recommendations. *European Archives of Paediatric Dentistry*, 2020, vol. 21, pp. 543–556. DOI: <https://doi.org/10.1007/s40368-020-00547-5>
25. Slayton R. L., Urquhart O., Araujo M. W. B., Fontana M., Guzmán-Armstrong S., Nascimento M. M., Novy B. B., Tinanoff N., Weyant R. J., Wolff M. S., Young D. A., Zero D. T., Tampi M. P., Pilcher L., Banfield L., Carrasco-Labra A. Evidence-based clinical practice guideline on nonrestorative treatments for carious lesions: A report from the American Dental Association. *The Journal of the American Dental Association*, 2018, vol. 149, iss. 10, pp. 837–849. DOI: <https://doi.org/10.1016/j.adaj.2018.07.002>

Поступила в редакцию / Received 19.02.2025

Принята к публикации / Accepted 18.06.2025

Опубликована / Published 02.03.2026